

Synthesis, characterization, and properties of copolymers of acrylamide with sodium 2-acrylamido-2-methylpropane sulfonate with nano silica structure

Haipeng Xin · Dun Ao · Xiaojin Wang · Yuejun Zhu · Jian Zhang · Yebang Tan

Received: 22 February 2014 / Revised: 17 November 2014 / Accepted: 10 January 2015 / Published online: 25 January 2015
© Springer-Verlag Berlin Heidelberg 2015

Abstract A novel water-soluble poly(acrylamide-co-sodium 2-acrylamido-2-methylpropane sulfonate) was synthesized by the emulsion copolymerization of acrylamide with sodium 2-acrylamido-2-methylpropane sulfonate using triethoxy(vinyl)silane modified nano silica as cross-linking agent. The structure, composition, thermal stability, and molecular weight of these copolymers were characterized by ¹HNMR spectrum, infrared spectra, elemental analysis, thermal gravimetric analysis, and light scattering. Static light scattering measurements showed that the copolymers had relatively high molecular weight ($M_w > 4 \times 10^6 \text{ g mol}^{-1}$). The solution properties of the copolymers were studied by viscosity measurement. The copolymers with nano silica structure possessed better viscosity properties and degradation resistance than linear copolymer. And the optimal feeding weight of modified nano silica was 0.10 g to obtain the lower crosslinked copolymer with effective thickening properties, temperature, and tolerance as well as salt resistance, indicating its potential application in enhanced oil recovery.

Keywords Water-soluble copolymer · Lower crosslinked polymer · Temperature tolerance · Shearing tolerance · Salt resistance

H. Xin · D. Ao · X. Wang · Y. Tan (✉)
School of Chemistry and Chemical Engineering, Shandong University, 250100 Jinan, China
e-mail: ybtan@sdu.edu.cn

H. Xin · D. Ao · X. Wang · Y. Tan
Key Laboratory of Special Functional Aggregated Materials,
Ministry of Education, Shandong University, 250100 Jinan, China

Y. Zhu · J. Zhang
Technology Research Department, CNOOC Research Center, State
Key Laboratory of Offshore Oil Exploitation, 100027 Beijing, China

Introduction

In recent years, nano structure organic–inorganic composites based on organic polymer and inorganic nano minerals play an important role in preparation of high-performance materials because organic materials have good process ability but poor mechanical properties, while inorganic materials have better high-temperature stability, durability, and electrical conductivity, which can enhance the mechanical strength of organic materials [1]. Thus, the polymer/nano composites have attracted great interest of researchers because of remarkable improvement in materials properties when compared with pure polymer. For hydrogel, film, and composite, these improvements include high module, higher mechanical strength, increased tensile strength, heat resistance, and decreased elongation at break and gas permeability [2–4]. Shengfang Li [2] prepared a series of poly(acrylic acid-co-acrylamide) (PAA)/SiO₂ hybrid hydrogels by in situ frontal polymerization. The velocity (V_f) and the highest front temperature of hydrogel were positively correlated with the concentration of SiO₂ nano particles. The prepared PAA/SiO₂ hybrid hydrogel also had high pH sensitivity and it exhibited a high compressive strength while remaining a high swelling ratio. The maximum of compressive strength and swelling ratio of the hybrid hydrogel may reach 42.6 and 17.8 kPa, respectively, which was much higher than that of pure PAA hydrogel. Ki Hong Kim [5] synthesized poly(styrene-co-acrylonitrile) (SAN)/multiwalled carbon nano tube (MWCNT) composite using polythiophene-graft-poly(methyl methacrylate) (PMMA) as compatibilizer. SAN/MWCNT nano composites in the presence of the compatibilizer show dramatically improved mechanical properties even with the addition of a very small amount (0.01 wt%) of MWCNT.

The solution properties of aqueous polymer solution could as be enhanced by injecting inorganic nano particles, and

silica nano particle is widely used. Ali Maghzi [6] used solutions of polyacrylamide and dispersed silica nano particles (DSNP) in polyacrylamide with different salinities as the injectants to examine the effect of silica nano particles on the polyacrylamide performance in oil recovery. The results showed that viscosity of silica nano suspension in polyacrylamide was higher than that of polyacrylamide solution at the same salinity. This increase in viscosity becomes more noticeable by increasing the silica nanoparticles concentration. Dingwei Zhu [7] mixed silica nanoparticle suspension and hydrophobically associating polyacrylamide (HAPAM) solution to prepared organic/inorganic hybrid aqueous solutions, and examined their rheological behaviors in both pure water and brine in comparison with HAPAM. It was found that HAPAM/silica hybrid exhibits viscosity enhancement in aqueous solution and better heat- and salt-tolerances than HAPAM due to the formation of micro cross-linking structure. Meanwhile, their long-term thermal stability is also improved.

However, high surface energy cause the nanoparticles to easily agglomerate, therefore, it is difficult to disperse the nano-SiO₂ in polymer matrix. To solve this problem, nano silica must be modified. Chemical modification of the nano silica particle can be achieved through a reaction between the hydroxyl groups on the silica surface and modifier. This modification decreases the amount of hydroxyl groups on the silica surface and leads to the particles with hydrophobic surface. Consequently, the inorganic nanoparticles may acquire better dispersibility and compatibility in the polymer matrix [8]. Nowadays, several methods are used to modify nano SiO₂ particles. Normal alcohols [9, 10], coupling agents [11–13], and polymer grafting [14–16] are mostly applied in which, silica surface modified with silane coupling agents to improve adhesion between the particles and the polymer is very effective [17]. The coupling agent can react with OH groups of silica surface, and an attached functionalized alkyl chain is more compatible with the polymer than the bare surface of the silica.

In this work, we modified nano silica with triethoxy(vinyl)silane to prepare nano silica with vinyl group on its surface. Then, acrylamide and sodium 2-acrylamido-2-methylpropane sulfonate were copolymerized with the surface vinyl group of modified nano silica via emulsion copolymerization, and water-soluble copolymer with nano silica structure was obtained. The copolymer was characterized by ¹HNMR spectrum infrared spectra, thermogravimetric analyses, light scattering, and viscosity measurements.

Experimental

Materials

Sodium 2-acrylamido-2-methylpropane sulfonate (AMPS) of chemical grade was obtained from Shanghai Darui Fine

chemical Co., Ltd. Sodium dodecyl sulfate (SDS), ammonium persulfate (APS), tetramethylethylenediamine (TMEDA), acrylamide(AM), triethoxy(vinyl)silane, ethanol, NaOH, HCl (37 %), and NaCl were obtained from Sinopharm Chemical Reagent Co., Ltd. (Shanghai, China). Nano silica of chemical grade was obtained from Cabot Corporation. All reagent, unless specially specified, were of analytical grade and were used without further purification. The water used was distilled for three times.

Modification of nano SiO₂

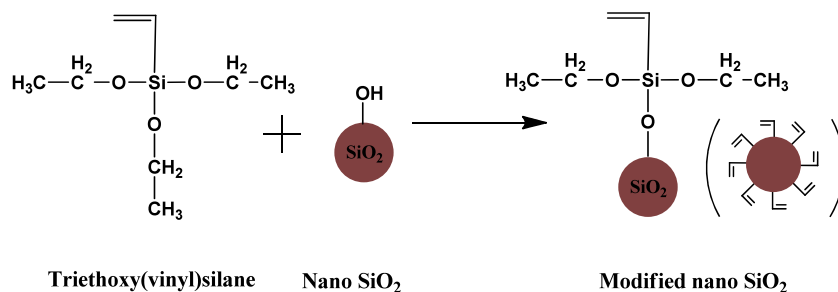
Surface modification of nano silica by triethoxy(vinyl)silane was achieved as shown in Fig. 1. Triethoxy(vinyl)silane (8.56 g, 0.045 mol) was initially added to ethanol (1000 mL) and the mixture stirred for 1 h. Nano silica (100 g) was then added to the mixture and heating reflux for 12 h. Resulting product was filtered after cooling to room temperature, washed by ethanol for three times and dried under vacuum for 24 h to give white crystalline solid (94.4 g, 87 %).

Synthesis of linear and lower crosslinked copolymer

One linear copolymer and three lower crosslinked copolymers using modified nano SiO₂ as lower cross-linking agent were prepared by free radical copolymerization in emulsion solution where the total monomer concentration was held constant 0.5 mol/L. SDS was dissolved in distilled water. Then AM, AMPS, and nano SiO₂ with designed mixture ratio were dropped into the SDS solution. The copolymerization was initiated by 0.6 mmol L⁻¹ of APS and 0.6 mmol L⁻¹ of TMEDA at 35 °C and pH 7.5 under nitrogen atmosphere (Fig. 2). After 4 h, the emulsion was precipitated by ethanol, and washed by ethanol for six times and mixture of water/ethanol (3:7, v/v) for three times to remove emulsifier and unreacted monomers. The product was dried in vacuum at 50 °C for 48 h.

Thermal and shearing degradation of copolymer solution

The copolymer solutions with concentration of 0.2 wt% were prepared. Each solution was divided into two equal parts, one part of which was thermal degradation at designed temperature for 0, 2, 4, 6, and 8 h, respectively. Four sealed high-pressure reactors inside lining polyfluortetraethylene were used during the thermal degradation in order to obtain the desired temperature, which was 85 °C. The other part was shearing degradation at 5000 r/min using warring blender for 0, 2, 4, 6, 8, and 10 min, respectively.

Fig. 1 Modification of nano SiO₂

Characterization

All ¹H-NMR experiments were performed on a Bruker AVANCE-400 NMR spectrometer. D₂O was used for field-frequency lock, and the observed ¹H chemical shifts were reported in parts per million (ppm) relative to an internal standard (TMS, 0 ppm).

Fourier transform infrared (FTIR) spectra of the dried samples in KBr pellets were recorded at room temperature (in the range 4000–400 cm⁻¹) using a Bruker Tensor 27 spectrometer.

Thermogravimetric analyses (TGA) of the dried samples were performed using a Mettler Toledo TGA/DSC 1 in the temperature range 30–700 °C under a nitrogen atmosphere, with heating performed at a rate of 10 °C min⁻¹.

Static light scattering (SLS) measurements were performed on a DAWN HELEOS light scattering instrument (Wyatt Technology). The system light source was a linearly polarized gallium arsenide (GaAs) laser (658 nm). The laser is positioned so that the incident beam was vertically polarized. Zimm plots were obtained using Astra software. The samples were examined in 0.1 mol/L NaCl solutions and filtered with a 0.2-μm filter (Millipore). A differential refractive index detector (Optilab-rEX) was used to measure the differential refractive indices (dn/dc) of copolymer solutions at 658 nm and 25 °C.

Dynamic light scattering (DLS) measurements were performed on a multi-angle laser photometer equipped with a linearly polarized gallium arsenide (GaAs) laser ($\lambda=658$ nm;

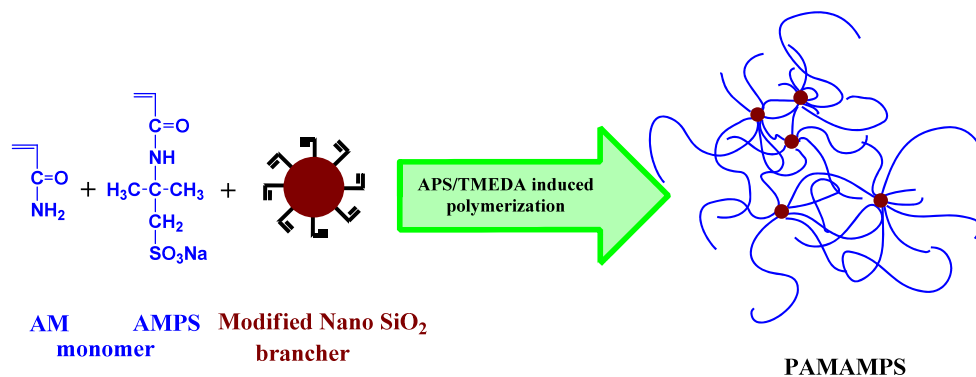
Wyatt Technology Co. DAWN HELEOS), which were conducted at a scattering angle of 99 °. In DLS, the Laplace inversion of each precisely measured intensity–intensity–time correlation function $G^{(2)}(t, q)$ in the self-beating mode could result in a line width distribution $G(\tau)$ [18]. For a pure diffusive relaxation, $G(\tau)$ can be converted to a translational diffusion coefficient distribution $f(R_h)$ by the Stoke–Einstein equation. In this study, the CONTIN Laplace inversion algorithm in the correlator was used [19]. All the solutions were filtered through Millipore 0.8-μm membranes before the DLS measurements.

The viscosity measurements were carried out on a HAAKE RS75 rheometer (Germany) with coaxial cylinder sensor system (Z41 Ti). The viscosity measure was carried out at shear rates of 7.34 s⁻¹ maintained at (25.0±0.1)°C.

Results and discussion

Characterization of the copolymer

The formation of copolymers was confirmed by ¹H-NMR spectrum in Fig. 3. As it was shown, methylene proton ($-CH_2-$) and methine proton ($-CH-$) in copolymer backbone contributed to the signal at around 1.5–1.9 and 2.0–2.5 ppm while methylene proton ($-CH_2-$ of $-CH_2SO_3^-$) of AMPS appeared at 3.0–3.5 ppm. The peak at 1.3–1.5 ppm consisted of chemical shift of the methyl protons ($-CCH_3$) of AMPS. The

Fig. 2 Synthesis route of the copolymer

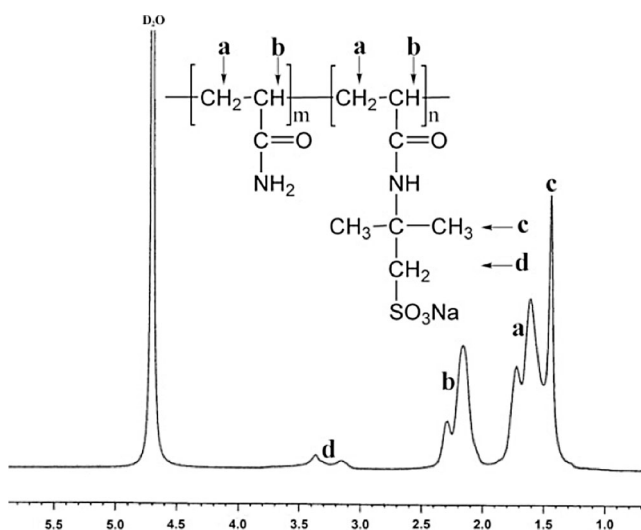


Fig. 3 $^1\text{H-NMR}$ spectrum of PAMAMPS

characteristic peaks to the protons of AM and AMPS indicated the linking of AM and AMPS monomer to the polymer backbone, and the monomer ratio of AM and AMPS in the copolymers were given in Table 1. As evidence from Table 1, the AMPS incorporations do not match with the feeding ratio; the mole percent AMPS incorporated in copolymers were always found to be less than the mole percent in the feed.

Figure 4 presents the IR spectra of nano SiO_2 , modified nano SiO_2 and copolymer. Comparing to nano SiO_2 , the absorption band around 958 cm^{-1} decreased to almost disappearing while two new absorption bands around 2925 and 2900 cm^{-1} in modified nano SiO_2 indicating that hydroxyl group react with the triethoxy(vinyl)silane in the modification of nano SiO_2 . Main assignments of absorption bands of the copolymer are as follows: (1) 3430 cm^{-1} , OH stretching (H_2O); (2) 3200 cm^{-1} , symmetric NH_2 stretching (amide group); (3) 2925 cm^{-1} , CH_2 bending; (4) 2900 cm^{-1} , CH_3 bending; (5) 1670 cm^{-1} , symmetric $\text{C}=\text{O}$ stretching (amide group); (6) 1560 cm^{-1} , symmetric $\text{C}=\text{O}$ stretching (carboxyl group); (7) 1460 cm^{-1} , CH_2 bending (amide group); (8) 1400 cm^{-1} , C-N-H bending (amide group); (9) 1300 cm^{-1} ,

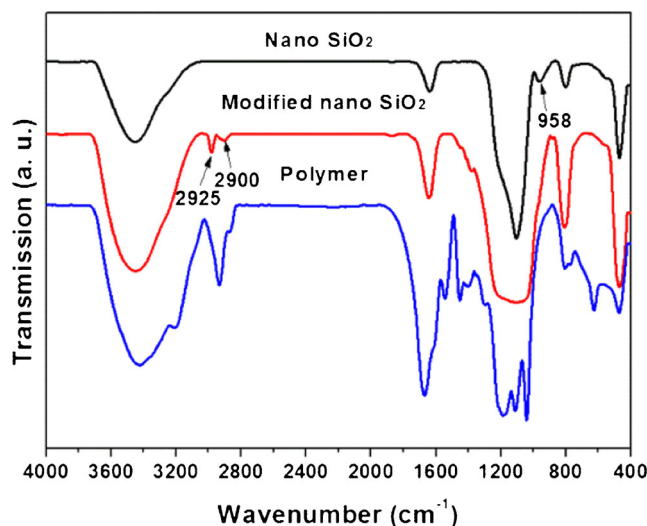


Fig. 4 IR spectra of nano SiO_2 , modified nano SiO_2 , and copolymer

C-N stretching (amide group); (10) 1180 cm^{-1} , SO_3 antisymmetric stretching (sulfonyl group of AMPS); (11) 1110 cm^{-1} , Si-O-Si antisymmetric stretching; (12) 1060 cm^{-1} , SO_3 symmetric stretching (sulfonyl group of AMPS); (13) 804 cm^{-1} , Si-O symmetric stretching; (14) 630 cm^{-1} , S-O bending (sulfonyl group of AMPS) and (15) 474 cm^{-1} , Si-O bending.

TGA and DTGA curves of copolymers are shown in Fig. 5. The thermogram of PAMAMPS-1 showed three steps during its mass loss. The first weight loss, at $40\text{--}160\text{ }^\circ\text{C}$, was related to moisture removal, with the sample losing 15.9 % of its weight. The second weight loss (the sample lost 24.8 % of its weight), at $270\text{--}350\text{ }^\circ\text{C}$, was attributed to the thermal decomposition of the amide side groups, which leads to the release of ammonia and other gaseous species from the polyacrylamide structure formed during the decomposition of PAMAMPS-1 [20]. In the third step, a sharp weight loss (26.1 %) occurred at $350\text{--}470\text{ }^\circ\text{C}$, which may have been due to copolymer backbone degradation, and the final decomposition temperature was observed to be $530\text{ }^\circ\text{C}$. The thermograms of PAMAMPS-2 and PAMAMPS-3 showed that less

Table 1 Characteristics of the copolymers

Sample	AM ^a (mol%)	AMPS ^a (mol%)	Modified nano SiO_2 (g)	AM ^b (mol%)	AMPS ^b (mol%)	Apparent viscosity ^{c,d} (mPas)	Yield (%)
PAMAMPS-1	80	20	0	82.3	17.7	122.16	92.1
PAMAMPS-2	80	20	0.05	82.4	17.6	130.90	93.2
PAMAMPS-3	80	20	0.10	82.2	17.8	160.15	92.7
PAMAMPS-4	80	20	0.15	82.4	17.6	130.88	94.0

^a Mol% monomer present in the feed ratio

^b Mol% monomer content in the copolymers, measured by $^1\text{H-NMR}$

^c The shearing rate for texting the apparent viscosity is 7.34 s^{-1}

^d The concentration of every sample is 0.2 wt%

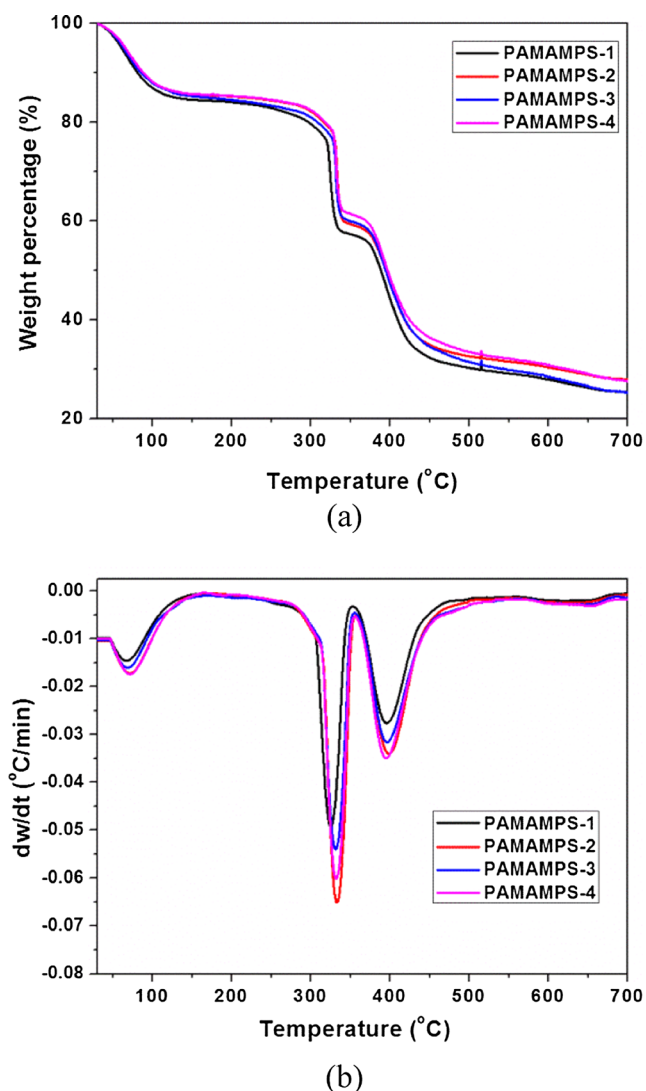


Fig. 5 TGA (a) and DTGA (b) curves of the copolymers

weight was lost (both of which are 14.9 %) in the temperature range 40–160 °C compared with that lost from PAMAMPS-1, which indicates that it had more bound water and a more hydrophilic polymer network [21]. PAMAMPS-2 and PAMAMPS-3 lost 23.0 and 22.8 % of weight at 275–355 °C while they lost 26.0 and 23.8 % of weight at 475–530 °C, respectively. The final decomposition temperature of both samples was also observed to occur at 530 °C. The thermogram of PAMAMPS-4 shows an almost similar thermal degradation pattern as other samples. Less weight was also lost (13.5 %) in the temperature range 40–160 °C compared with that lost from other samples. Moreover, the sample lost 22.6 and 28.7 % of its weight at 275–355 and 475–530 °C, respectively. The final decomposition temperature was also observed to occur at 530 °C.

Therefore, up to 530 °C, the char yield of samples from high to low was in order of PAMAMPS-4, PAMAMPS-3,

PAMAMPS-2, and PAMAMPS-1 indicating that the addition of nano SiO₂ make polymer possess better heat tolerance. Although samples performed similar thermal degradation pattern, the most rapid decomposing temperature of PAMAMPS-1 and other samples are different at 275–355 °C. The most rapid decomposing temperature of PAMAMPS-1 is 323 °C as shown in Fig. 5b. And when it comes to copolymers with nano silica structure (PAMAMPS-2, PAMAMPS-3, and PAMAMPS-4), the most rapid decomposing temperature is about 332–335 °C, which is nearly 10 °C above than PAMAMPS-1. Thus, we suggest that the addition of nano silica structure may contribute to enhance the thermal stability of polymer samples.

In SLS measurement, we were able to obtain weight-average mole mass M_w , the second-order virial coefficient A_2 , and the mean square radius $\langle R_g^2 \rangle$ of polymer chains from the angular dependence of the excess absolute scattering intensity, known as the Rayleigh ratio $R(\theta)$, on the basis of

$$\frac{K^*C}{R(\theta)} = \frac{1}{M_w} \left(1 + \frac{1}{3} \langle R_g^2 \rangle q^2 \right) + 2A_2C \quad (1)$$

Where $K^* = 4\pi(dn/dc)^2 n_0 / (N_A \lambda_0^4)$, and $q = (4\pi n_0 / \lambda_0) \sin(\theta/2)$, with n_0 , dn/dc , λ_0 , and θ being the solvent refractive index, the specific refractive index increment, the wavelength of the incident light in vacuum, and the scattering angle, respectively [22].

The molecular weight determination of the copolymers was performed in 0.1 mol L⁻¹ NaCl aqueous solution. For linear and branched copolymers in 0.1 mol L⁻¹ NaCl aqueous solutions, the values of dn/dc are 0.1338 and 0.1442, respectively. Figure 6 shows a typical static Zimm plot of PAMAMPS-1 in 0.1 mol L⁻¹ NaCl aqueous solution, where C ranges from 1×10^{-5} to 8×10^{-5} g mL⁻¹. Using the

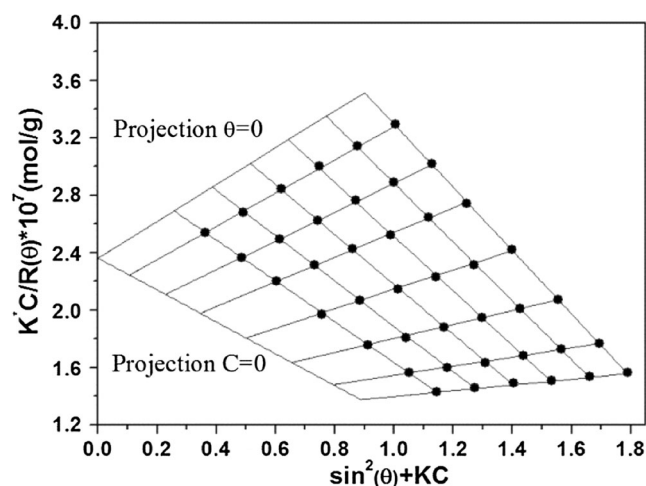


Fig. 6 Zimm plot of PAMAMPS-1 in 0.1 mol L⁻¹ NaCl solution

projection $\theta=0$ and $C=0$, the values of M_w , R_g , and A_2 calculated on the basis of Eq. 1 are listed in Table 2. The molecular weights of copolymers are similar; ranging from 4.18×10^6 to $4.73 \times 10^6 \text{ g mol}^{-1}$, so a meaningful comparison of their rheological behavior can be made. It is difficult to draw a general trend about the evolution of the second virial coefficient A_2 as a function of the nano SiO_2 content. However, one can note that A_2 is always negative, indicating that 0.1 mol L^{-1} NaCl aqueous solution is not a good solvent for all copolymers. The trend in R_g was paralleled by nano SiO_2 feeding content, which could be affected by the content of nano SiO_2 in copolymers. Also as expected, one observes that R_g decreased with the increasing the content of nano SiO_2 , which was caused by the enhancement of branching degree.

Aggregation behavior of the copolymer in solution by light scattering measurement

The average hydrodynamic radius (R_h) of copolymers in solution, obtained from dynamic light scattering (DLS) measurement, is an important physical parameter, because a lot of information about the size of molecules and the state of interaction between molecules could be obtained from the DLS analysis. The distribution of the hydrodynamic radius and the average hydrodynamic radius of copolymers in 0.1 mol/L NaCl solution was obtained by DLS as shown in Fig. 7 and Table 2. R_h decreased with the increase of nano SiO_2 . The main reason may be that the risk of crossing increased with the increase of nano SiO_2 concentration which would also increase the segment density as well as the resistance to the monomer diffusing into branching point resulting in the decrease of copolymer size.

Another useful information of light scattering is to determine the conformation of copolymers when both the R_g and R_h are measured. The ratio of R_g to R_h , as shown in Table 2, reveals the shape of a polymer. For solid spheres, the ratio is 0.77; for random coil polymers, the ratio equals to 1.50. In our test, the ratio of R_g/R_h for

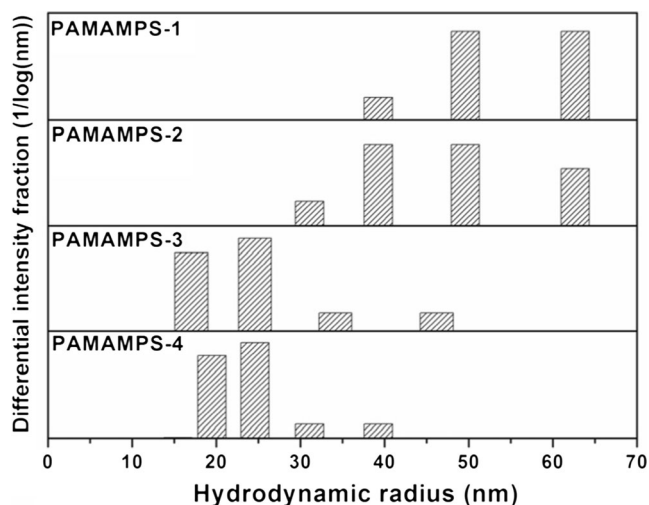


Fig. 7 R_h of copolymers in 0.1 mol L^{-1} NaCl solution

PAMAMPS-1 sample is 1.54 close to the value for a polymer with a linear chain conformation. The ratio for PAMAMPS-2 and PAMAMPS-3 was found to be nearly 1 (actually, it varies from 1.22 to 0.95), indicating that these systems exhibit a behavior between hard spheres (ratio=0.77) and flexible polymers (ratio=1.50). Note that for particles with spherical symmetry, this ratio assumes its maximum value of 1 in the case of hollow spheres (e.g., vesicles); the present PAMAMPS-4 polymer, as well as the polymer coils, are not truly spherically symmetric, and thus, a logical analogy to hollow spheres is not fully justifiable in this respect. On the other hand, it is possible that the PAMAMPS-2 and PAMAMPS-3 might have a wedge-like shape [23]. The ratio for this PAMAMPS-4 sample is 0.84 close to the value for hard spheres (ratio=0.77) indicating its conformation of high-branched structure.

The effect of salinity on viscosity of copolymer solution

The effect of salt concentration on apparent viscosity of copolymer solution was shown in Fig. 8. From the results, it is indicated that the apparent viscosity of all samples decreased while increasing salt concentration from 0 to 1 mol L^{-1} due to the fact that the electric double layer of copolymers were compressed by salt ions. However, the relative viscosity of PAMAMPS-1 decreased to 49.2 % in the salt concentration increasing procedure while the relative viscosity of PAMAMPS-2 and PAMAMPS-3 decreased to 79.5 and 89.5 %, respectively, while the relative viscosity of PAMAMPS-4 decreased to 87.9 %. The results showed that the branched copolymers kept higher apparent viscosity and lower decreasing rang than linear copolymer. And the viscosity percentage was parallel to the feeding content of modified

Table 2 Light scattering data for the copolymers in 0.1 mol L^{-1} NaCl solution

Sample	M_w^a (10^6 g mol^{-1})	R_g^a (nm)	A_2^a ($10^{-3} \text{ mol mL g}^{-2}$)	R_h^b (nm)	R_g/R_h
PAMAMPS-1	4.20	86.5	-2.14	56.2	1.54
PAMAMPS-2	4.45	54.3	-3.37	44.5	1.22
PAMAMPS-3	4.73	33.4	-4.01	35.2	0.95
PAMAMPS-4	4.18	23.4	-2.46	27.9	0.84

^a Determined via static light scattering

^b Determined via dynamic light scattering

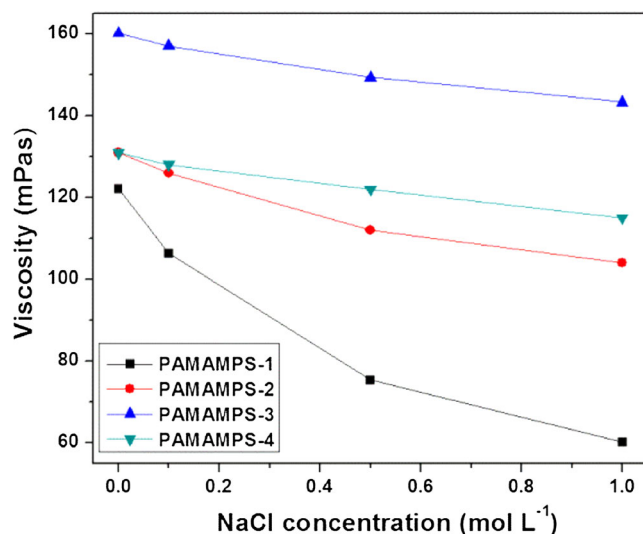
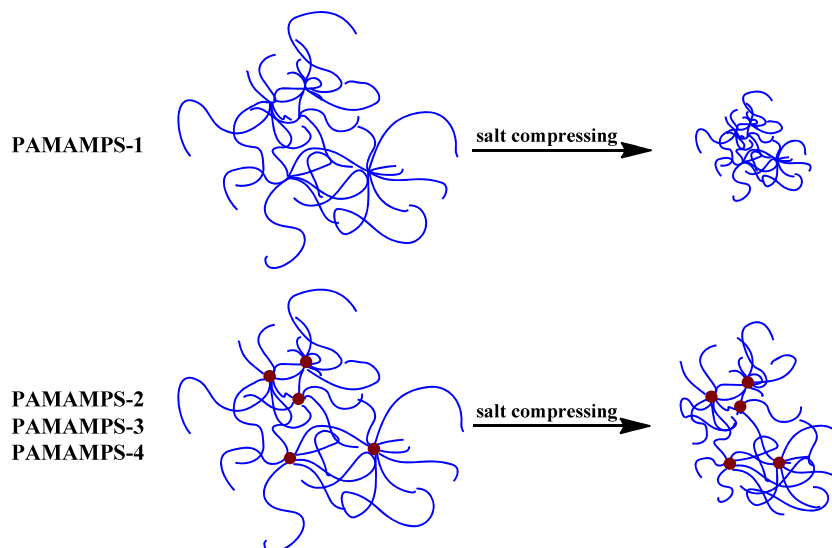


Fig. 8 Viscosity of the copolymers in saline solutions

nano silica implying that silica treatment improved the ability of copolymers to maintain viscosity under salinity stress.

The scheme model of copolymers compressed by salt was given as Fig. 9. Linear copolymer PAMAMPS-1 chains were in stretched conformation in aqueous solution. When salt ions were added, the chains were compressed and the gyration radius of copolymer coils decreased sharply inducing the significant decrease of viscosity. When it comes to copolymers with nano silica structure (PAMAMPS-2, PAMAMPS-3, and PAMAMPS-4), the gyration radius of copolymer coils decreased slightly due to the existence of nano silica particle. Although copolymer chains could be compressed by salt ions, inorganic nano particle was impregnable. Thus, gyration radius of copolymer coils with nano silica structure could still maintain a larger size and finally induced better viscosity percentage than PAMAMPS-1.

Fig. 9 The scheme model of the copolymers compressed by salt



The effect of shearing and thermal degradation on viscosity of copolymer solution

The effect of shearing on apparent viscosity of copolymer solution was shown in Fig. 10a. From the results, it is indicated that the apparent viscosity of all copolymers decreased during the degradation due to the scission of backbones. The relative viscosity of PAMAMPS-1 decreased to 65.7 %. The relative viscosity of PAMAMPS-2 and PAMAMPS-3 decreased to 83.1 and 90.3 %, respectively. And the relative viscosity of PAMAMPS-4 decreased to 78.6 %. The results showed that the branched copolymers kept higher apparent viscosity and lower decreasing range than linear copolymer. The main reason may be that appropriate branching structure could contribute to shearing endurance. At the mean time, PAMAMPS-3 kept the highest apparent viscosity all along the shearing procedure which indicated that the optimal feeding content of modified nano silica was 0.10 g.

Apparent viscosity of copolymer solution also decreased with the increase of thermal aging time as shown in Fig. 10b. For thermal degradation at 85 °C, PAMAMPS-3 also kept the highest apparent viscosity all along as well as shearing degradation which indicated PAMAMPS-3 performed good thermal endurance with content of modified nano silica 0.10 g.

Through the study of shearing and thermal degradation, we predict the degradation model of copolymer samples as presented in Fig. 11. Random bond scission of linear (PAMAMPS-1) polymeric main chain backbone forming short chains was supposed to happen which would lead to the sharp decrease of apparent viscosity. Different from linear copolymer, degradation of branched copolymer deeply depended on its branching degree due to the

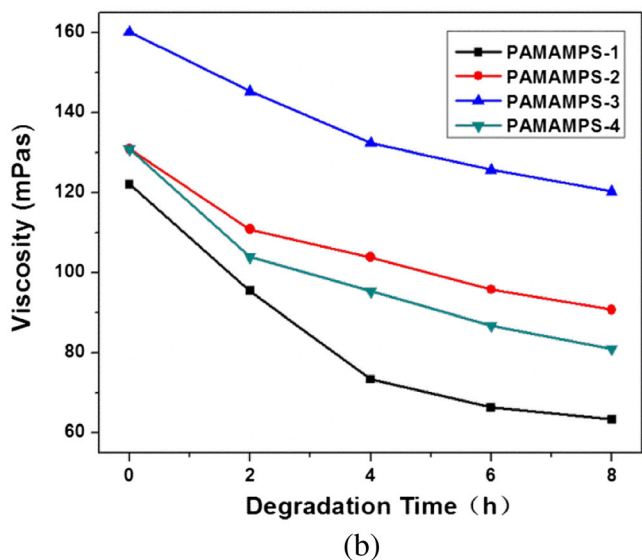
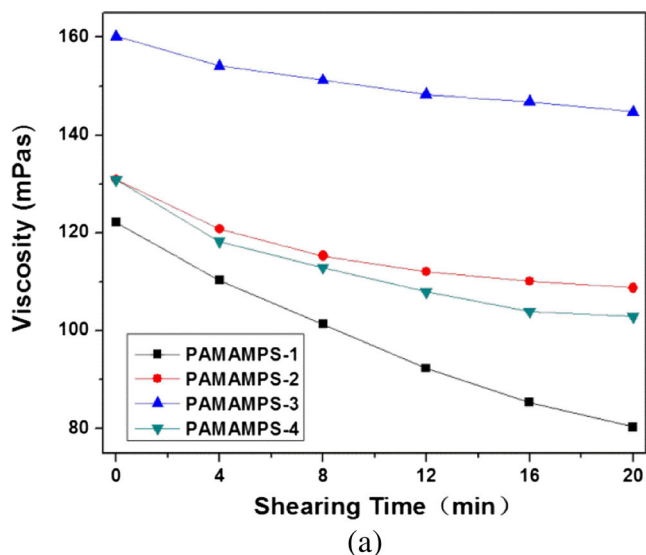


Fig. 10 Viscosity of the copolymers in shearing (a) and thermal (b) degradation procedure

random bond scission of the polymeric main chain backbone and branching point. Random bond scission of low-branched (PAMAMPS-2) polymeric main chain backbone, with small amount of branching point, primary formed long and short chains. These chains would be longer than those formed from linear polymer which meant that low-branched copolymer would perform better degradation endurance and keep higher apparent viscosity. The degradation of medium-branched copolymer (PAMAMPS-3) would be complicated due to the growing numbers of branching point. Some branching point would break up which induced the formation of long and short chains while some branching point kept stable inducing the formation of a secondary branched structure with

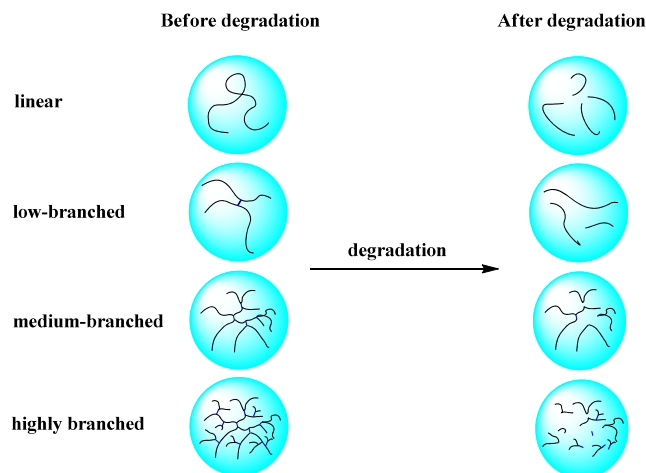


Fig. 11 The scheme route of the copolymer degradation

relatively high molecular weight than linear chain fragments. Thus, medium-branched polymer would perform quite good degradation endurance and keep high apparent viscosity all along the degradation procedure compared with linear and low-branched copolymer. The degradation of highly branched copolymer (PAMAMPS-4) is quite a contrast to medium-branched copolymer (PAMAMPS-3) owing to the existence of overmuch branching point which would hamper the free rotation of copolymer chain resulting in the markedly degradation of highly branched copolymer. Therefore, highly branched copolymer would perform bad degradation endurance even worse than linear copolymer which depended on the molecular weight and external degradation conditions.

The effect of temperature on viscosity of copolymer solution

As is well known, the increase of temperature can give to crimple of acrylamide copolymer molecules due to its dehydrating and destruction of the associational structure [24]. To further study the thermal stability of copolymers, viscosity measurement at different temperature from 25 to 65 °C was carried as shown in Fig. 12a.

It is reported that the relationship between apparent viscosity of copolymer solution and temperatures satisfies Arrhenius equation:

$$\eta_0(T) = A \exp(\Delta E_\eta / RT) \quad (2)$$

Where $\eta_0(T)$ is zero shear apparent viscosity and ΔE_η is the flow activation energy, with A , R , and T being a constant, the universal gas constant, and T is the temperature (in Kelvin) [25].

Flow activation energy, which could characterize the dependence of apparent viscosity on temperature, is a

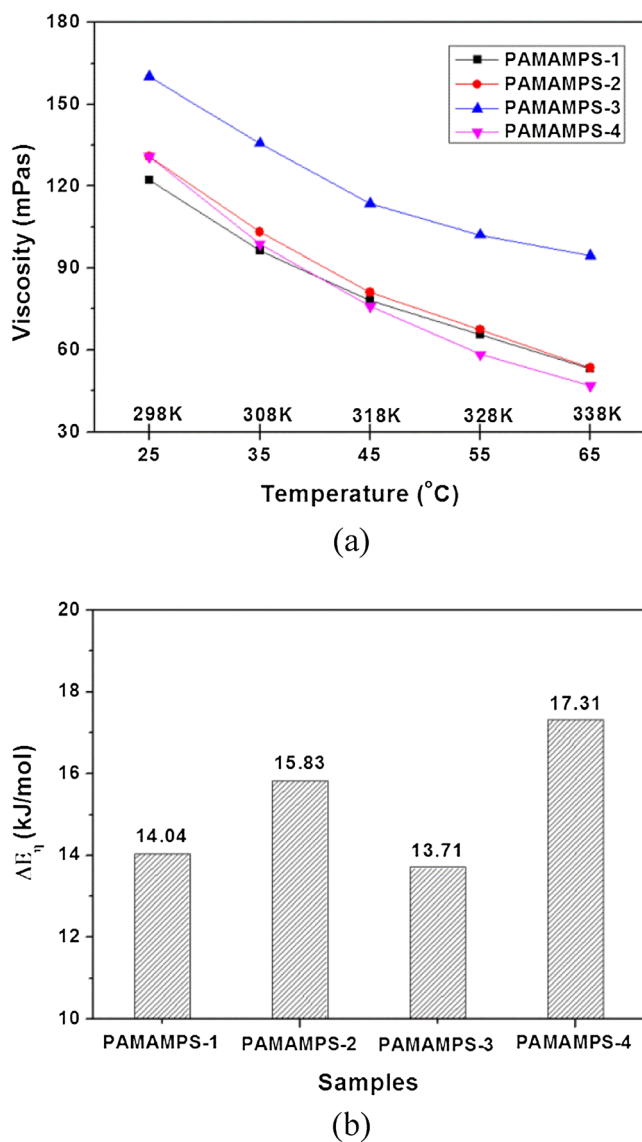


Fig. 12 The effect of temperature on the viscosity of the copolymer solution and flow activation energy of the copolymer solution

measurement of the least amount of energy needed for the flow unit overcome the barrier transferred from the original position to the “hole” near in the process of flow. As for polymer, chain segment is the flow unit indicating that ΔE_{η} of polymer is relative to polymer structure rather than molecular weight.

The Arrhenius plot was obtained by plotting the logarithm of the zero shear apparent viscosity, $\eta_0(T)$, versus the inverse temperature, $1/T$. The resulting negatively sloped line is useful for finding the missing components of the Arrhenius equation. Extrapolation of the line back to the y -intercept yields the value for $\ln A$. The slope of the line is equal to the negative flow activation energy divided by the gas constant, R , from which ΔE_{η} could be obtained as shown in Fig. 12(b). PAMAMPS-3 performed the lowest flow activation energy with a concentration of

0.2 wt% indicating that its apparent viscosity is less sensitively depend on temperature than other copolymers.

Conclusions

We prepared a linear poly(acrylamide-co-sodium 2-acrylamido-2-methylpropane sulfonate) and water-soluble poly(acrylamide-co-sodium 2-acrylamido-2-methylpropane sulfonate) with nano silica structure via aqueous emulsion polymerization. The structure, compositions and of copolymers were ascertained by $^1\text{H-NMR}$ and elemental analysis. The proper copolymers had relatively high molecular weight ($M_w > 4 \times 10^6 \text{ g mol}^{-1}$) with effective thickening properties, temperature tolerance, and resistance to shear force as well as salt compression. The copolymers branched by 0.10 g of modified nano silica possess the highest viscosity, temperature, and tolerance as well as salt resistance.

Acknowledgments The authors gratefully acknowledge the financial support from Major Research of Science and Technology, China (Grant No.2011ZX05024-004-08).

References

- Wu CS, Liao HT (2013) Characterization and antistatic behavior of SiO_2 -functionalized multiwalled carbon nanotube/poly(trimethylene terephthalate) composites. *J Polym Res* 20:253
- Li SF, Wang H, Huang W, Liu X (2014) Facile preparation of pH-sensitive poly(acrylic acid-co-acrylamide)/ SiO_2 hybrid hydrogels with high strength by in situ frontal polymerization. *Colloid Polym Sci* 292:107–113
- Wisniewska M (2011) The temperature effect on electrokinetic properties of the silica–polyvinyl alcohol (PVA) system. *Colloid Polym Sci* 289:341–344
- Etxeberria H, Zalakain I, Mondragon I, Eceiza A, Kortaberria G (2013) Generation of nanocomposites based on polystyrene-grafted CdSe nanoparticles by grafting through and block copolymer. *Colloid Polym Sci* 291:1881–1886
- Kim KH, Jo WH (2007) Synthesis of polythiophene-graft-PMMA and its role as compatibilizer for poly(styrene-co-acrylonitrile)/MWCNT nanocomposites. *Macromolecules* 40:3708–3713
- Maghzi A, Kharrat R, Mohebbi A, Ghazanfari MH (2014) The impact of silica nanoparticles on the performance of polymer solution in presence of salts in polymer flooding for heavy oil recovery. *Fuel* 123:123–132
- Zhu D, Han Y, Zhang J, Li X, Feng Y (2014) Enhancing rheological properties of hydrophobically associative polyacrylamide aqueous solutions by hybridizing with silica nanoparticles. *J Appl Polym Sci*. doi:10.1002/app.40876
- Zhang FA, Kang JS, Yu CL (2011) Effect of acrylic acid and hydroxyethyl methacrylate modified nano- SiO_2 particles on poly(methyl methacrylate-hydroxyethyl methacrylate) soap-free emulsion polymerization. *J Polym Res* 18:615–620

9. Fuji M, Takei T, Watanabe T, Chikazawa M (1999) Wettability of fine silica powder surfaces modified with several normal alcohols. *Colloid Surf A* 154:13–24
10. Qian XJ, Liu XH, Lu LD, Chen WJ, Wang X (2004) Surface modification of the nano-SiO₂ with 1-octylalcohol. *Chin J Inorg Chem* 20:335–338
11. Zhang L, Zhang DF (2005) Study on the surface modification and characterization of nano-SiO₂. *Russ J Inorg Chem* 50: 925–930
12. Li YP, Wang YQ, He WW, Chen ZQ, Zhang RY, Huang L (2006) Preparation and characterization of nano-SiO₂/acrylic resin composite latex. *Acta Polym Sin* 953–958
13. Gao JC, Zou J, Tan XW, Wang Y (2006) Characteristics and properties of surface coated nano-TiO₂. *Trans Nonferrous Met Soc China* 16:1252–1258
14. Bauer F, Sauerland V, Gläsel HJ, Ernst H, Findeisen M, Hartmann E, Langguth H, Marquardt B, Mehnert R (2002) Preparation of scratch and abrasion resistant polymeric nanocomposites by monomer grafting onto nanoparticles, 3. Effect of filler particles and grafting agents. *Macromol Mater Eng* 287:546–552
15. Yao L, Yang TL, Cheng SY (2008) Study of nano-silica/fluorinated acrylate copolymer hybrid emulsion and the polymerization kinetics. *Acta Polym Sin* 221–230
16. Zhao H, Sun RM, Luo YJ, Li J (2008) A novel method of hyperbranched poly(amide-ester) modifying nano-SiO₂ and study of mechanical properties of PVC/nano-SiO₂ composites. *Polym Compos* 29:1014–1019
17. Mehdi SK, Vahid HA, Said RR, Farid BS, Mohammad N, Hossein RM (2012) A study on the properties of PMMA/silica nanocomposites prepared via RAFT polymerization. *J Polym Res* 19:9793
18. Chu B (1974) *Laser light scattering*. Academic Press, New York
19. Provencher SW (1976) A Fourier method for the analysis of exponential decay curves. *Biophys J* 16:27–41
20. Caulfield MJ, Qiao GG, Solomon DH (2002) Some aspects of the properties and degradation of polyacrylamides. *Chem Rev* 102: 3067–3084
21. Saeidi A, Katbab AA, Vasheghani-Farahani E, Afshar F (2004) Formulation design, optimization, characterization and swelling behaviour of a cationic superabsorbent based on a copolymer of [3-(methacryloylamino)propyl]trimethylammonium chloride and acrylamide. *Polym Int* 53:92–100
22. Zimm BH (1948) The scattering of light and the radial distribution function of high polymer solutions. *J Chem Phys* 16:1093–1099
23. Asteriadi A, Sigel R, Vlassopoulos D, Meier G, Dorgan JR, Knauss DM (2004) Molecular control of the viscosity of model dendritically branched polystyrene solutions: from polymeric to colloidal behavior. *Macromolecules* 37:1016–1022
24. Xin X, Xu GY, Wu D, Li YM, Cao XR (2007) The effect of CaCl₂ on the interaction between hydrolyzed polyacrylamide and sodium strarate: Rheological property study. *Colloids Surf A* 305:138–144
25. Jie C, Che YJ, Cao XL, Zhang JC, Wang HY, Tan YB (2008) Rheological properties of poly(acrylamide-co-sodium acrylate) and poly(acrylamide-co-sodium vinylsulfonate) solutions. *J Cent South Univ Technol* 15:107–110